

Article

A Modified Equation for Thickness of the Film Fabricated by Spin Coating

Un Gi Lee ¹, Woo-Byoung Kim ², Do Hyung Han ² and Hyun Soo Chung ^{1,*}¹ Department of Mathematics, Dankook University, Cheonan 31116, Korea; leewg@dankook.ac.kr² Department of Energy Engineering, Dankook University, Cheonan 31116, Korea; woo7838@dankook.ac.kr (W.-B.K.); hans417@naver.com (D.H.H.)

* Correspondence: hschung@dankook.ac.kr

Received: 19 August 2019; Accepted: 10 September 2019; Published: 18 September 2019



Abstract: According to the equation for Newtonian fluids, the film thickness after spin coating is determined by five parameters: angular velocity, spin coating time, viscosity, density of the coating material, and initial thickness of the material before spin coating. The spin coating process is commonly controlled by adjusting only the angular velocity parameter and the coating time in the Newtonian expression. However, the measured coating thickness obtained is then compared to the theoretical thickness calculated from the Newtonian fluid equation. The measured coating thickness usually varies somewhat from the theoretical thickness; further details are described in Section 1. Thus, the Newtonian fluid equation must be modified to better represent the actual film thickness. In this paper, we derive a new formula for the spin coating film thickness, which is based on the equation for Newtonian fluids, but modified to better represent film thicknesses obtained experimentally. The statistical analysis is performed to verify our modifications.

Keywords: spin coating process; modified Newton's formula; statistical analysis; curve estimated function; polyhedron approximation

1. Introduction

In Ref. [1], Emslie, Bonner and Peck proposed differential equations in cylindrical polar coordinates to calculate the thickness of Newtonian liquid on a rotating disk. They took cylindrical polar coordinates (r, θ, z) rotating with the spinning disk at angular velocity W . The z dependence of the radial velocity v of the liquid at any point (r, θ, z) can be found by equating the viscous and centrifugal forces per unit volume:

$$-\eta \frac{\partial^2 v}{\partial z^2} = \rho W^2 r, \quad (1)$$

where η is the viscosity and ρ the density of the liquid. Equation (1) may be integrated employing the boundary conditions that $v = 0$ at the surface of the disk ($z = 0$) and $\partial v / \partial z = 0$ at the free surface of the liquid ($z = h$), where the shearing force must vanish. Hence,

$$v = \frac{1}{\eta} \left(-\frac{1}{2} \rho W^2 r z^2 + \rho W^2 r h z \right). \quad (2)$$

The radial flow q per unit length of circumference is

$$q = \int_0^h v dz = \frac{\rho W^2 r h^3}{3\eta}. \quad (3)$$

In order to obtain a differential equation for h we apply the equation of continuity,

$$r \frac{\partial h}{\partial t} = -\frac{\partial(rq)}{\partial r}. \quad (4)$$

Thus, via Equation (3),

$$\frac{\partial h}{\partial t} = -K \frac{1}{r} \frac{\partial}{\partial r} (r^2 h^3), \quad (5)$$

where $K = \frac{\rho W^2}{3\mu}$.

They obtained the solution which depends only on t . In this case, we have

$$\frac{dh}{dt} = -2Kh^3. \quad (6)$$

Hence, they obtained the general solution (7), the equation for thickness of the film fabricated by spin coating, describes the film thickness obtained after the spin coating process

$$h = \frac{h_0}{\sqrt{1 + \frac{4\rho W^2 h_0^2 t}{3\mu}}}, \quad (7)$$

where h_0 is the initial thickness of the coating material [1–4]. Note that the final thickness of the film is affected more by the angular velocity and time than by the other factors. Given that $W = \frac{\pi}{30} \times \omega$, where ω is the number of revolutions per minute (RPM), the final thickness h of the film can be treated as a two-variable function of t and ω [1–12].

Spin coating technology is useful in modern industrial society. However, it still relies on Formula (7), which was introduced in the 1950s, to determine spin coating film thickness. Many companies that deal with spin coating processes do not actually use the equation for thickness of the film fabricated by spin coating (7) to determine spin coating thickness, due to the considerable discrepancy between the theoretical and actual thickness values. Because of these differences in the spin coating process, the traditional equation for thickness of the film fabricated by spin coating (7) was not used, but rather the repetitive empirical formula has been used. Currently, many scholars are trying to reduce these differences [13,14]. The disadvantages of our approach is that the empirical formula must be refreshed whenever the experimental environment changes; additionally, this process tends to be costly and time-consuming. Thus, a new mathematical formula is needed to describe the spin coating process and resulting film thickness. In order to verify this, we are going to conduct an experiment to measure the final thickness in the spin coating process. The experimental environment is given as follows:

- (a) The viscous PDMS (Polydimethylsiloxane) coated on the glass (Sylgard 184, Dowcoating) is using the spin coating material.
- (b) The substrate of size $2 \times 2 \text{ cm}^2$ is used to measure the film thickness at the center of the substrate, and the substrate of size $3 \times 3 \text{ cm}^2$ is used to measure the overall thickness distribution of the PDMS film.

- (c) We fix the viscosity, density of coating material, initial thickness at 4000 cP, 965 kg/m³ and 0.105 cm. Then, the rotation time is fixed at 300 s and the experiment is performed in 500 RPM units from 500 to 6000 RPM.
- (d) The spin coating is performed by Spin coater ACE-200 (DongAh Trade Corp, Seoul, South Korea).
- (e) Finally, we measure all samples thickness and thickness distribution to step measurement by surface profiler DektakXT (Bruker, Karlsruhe, Germany).
- (f) Thickness measurement is performed by measuring the thickness when the stylus of the DektakXT passed through the coated film from the uncoated section of the substrate.
- (g) We focus on a coating thickness range of 4 to 20 μm using experimental limits of $\omega = 1000, 2000$ and 3000 and $t = 300, 450$ and 600 s. In these experimental conditions, the equation for thickness of the film fabricated by spin coating is given by the formula:

$$h(\omega) = \frac{1050}{\sqrt{1 + 0.00116671\omega^2}} (\mu\text{m}),$$

where μm is the micro meter, i.e., 1 μm = 10⁻⁶ m.

Remark 1. PDMS is a non-Newtonian fluid and, in [15], the authors pointed out that a study on the realistic flow for flattening of thickness through spin coating using non-Newtonian fluids. However, in [16], experiments were conducted with non-Newtonian fluids to study the applicability of non-Newtonian fluids to Newtonian fluid law. In this paper, the experiments were carried out using the most basic theory about the thickness of films made by the spin coating and non-Newtonian fluids. Based on the results, Equation (7) was used to modify the new equation.

After conducting the experiment, we can find that the measured thickness (MT) is slightly different from the theoretical thickness (TT). These differences are given by the Table 1 below.

Table 1. The thickness profile at each RPM and fixed time as 300 s.

RPM	TT (μm)	MT (μm)
500	61.38	52.99
1000	30.73	25.09
1500	20.49	15.36
2000	15.37	11.16
2500	12.30	8.53
3000	10.25	6.60
3500	8.78	5.30
4000	7.68	4.26
4500	6.83	3.92
5000	6.15	3.54
5500	5.59	2.80
6000	5.12	2.72

The existing equation for Newtonian fluids has five parameters: viscosity and density of material, spin coating speed and time, and initial height of the material before spin starting. Due to these various parameters, there is a difference in thickness to apply the existing equation to actual experiments. Equation (7) is an ideal equation containing at least five variables. However, it does not include variables such as the surface tension of the substrate. These variables and experimental conditions affect the difference between the theoretical thickness and the actual thickness.

This paper introduces a modified equation for thickness of the film fabricated by spin coating like Equation (7) that is based on curve estimation and polyhedron approximation. The mathematical accuracy of the proposed formula is examined through a statistical analysis of thickness [17,18]. Finally, the modified Newtonian fluid formula is used to construct an Excel-based thickness calculator for spin

coating applications. Here, we use the Statistical Package for Social Science (SPSS software, IBM Corp., Armonk, NY, USA) to estimate the curve and the polyhedron that best matches the experimental data.

2. A Modified Equation for Thickness of the Film Fabricated by Spin Coating via the Curve Estimation

In this section, we establish the modified equation for thickness of the film fabricated by spin coating in the spin coating process as a curve estimated function, and begin by referring to Table 1 above. From Table 1 in Section 1, the thickness calculated using the conventional theoretical equation and the thickness obtained using a repetitive empirical formula differ considerably. Thus, the theoretical equation must be modified with a curve estimated function to provide a more accurate calculated film thickness.

2.1. Fixed Time at 300 s

The estimation method is carried out through three steps. We shall explain this step by step.

Step 1. We use the Curve Estimation of the regression analysis from the SPSS to make a curve estimate for the MT value of Table 1 above. There are 11 models available in the curve estimation menu. Among these, we select five models with the possibility of being suitable for MT data. They are Logarithmic, Inverse, Quadratic, Cubic and Power models. The results of the analysis are as follows (Figure 1).

Model Summary and Parameter Estimates

Dependent Variable: 300s MT

Equation	Model Summary					Parameter Estimates			
	R Square	F	df1	df2	Sig.	Constant	b1	b2	b3
Logarithmic	.863	63.072	1	10	.000	151.978	-17.787		
Inverse	.999	15446.775	1	10	.000	-2.395	27472.245		
Quadratic	.859	27.359	2	9	.000	52.493	-.024	2.720E-006	
Cubic	.956	57.474	3	8	.000	71.442	-.053	1.355E-005	-1.111E-009
Power	.997	3398.438	1	10	.000	111118.372	-1.219		

The independent variable is RPM.

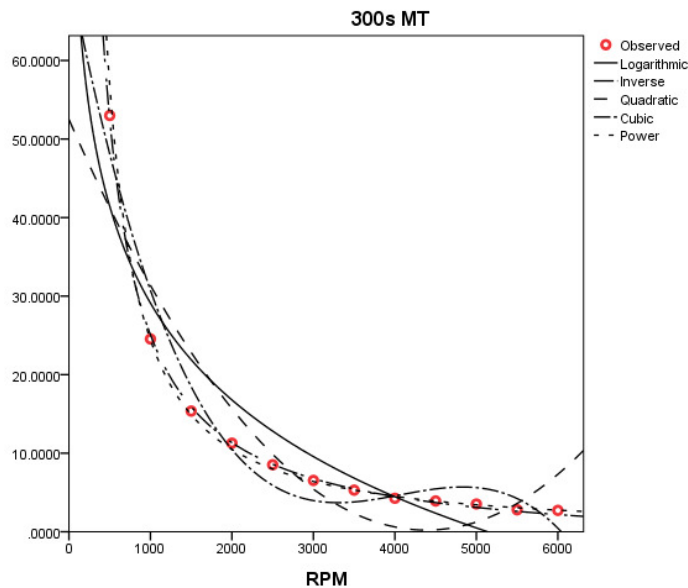


Figure 1. Curve estimation for 300 s MT.

As shown in Figure 1 above, we can choose the power model and the inverse model based on the value of the coefficient of determination. The estimated functions are given by the formulas

$$\text{power : } h_{power}(\omega) = 111118.372 \omega^{-1.2193}$$

and

$$\text{inverse : } h_{inverse}(\omega) = -2.3948 + \frac{27472.2453}{\omega}.$$

Both estimated functions are suitable for reducing the difference in film thickness mentioned above. It is also possible to select and use what is applicable to each company. Then, we obtain Table 2 involving the estimated function value and R^2 (coefficient of determination) value with respect to the MT value.

Table 2. Estimated function value and R^2 value for the MT value.

RPM	TT	MT	$h_{inverse}$	h_{power}
500	61.375	52.991	52.550	56.876
1000	30.727	24.541	25.077	24.428
1500	20.490	15.357	15.920	14.900
2000	15.368	11.280	11.341	10.492
2500	12.295	8.528	8.594	7.992
3000	10.246	6.530	6.763	6.399
3500	8.783	5.301	5.454	5.303
4000	7.685	4.264	4.473	4.506
4500	6.831	3.920	3.710	3.903
5000	6.148	3.536	3.100	3.433
5500	5.589	2.801	2.600	3.056
6000	5.123	2.718	2.184	2.748
R^2			0.999	0.997

As shown in Table 2 above, MT value and estimated function value are each somewhat different. To compensate for this, we implement the next step.

Step 2. Let E_{300} denote the difference of the TT value and the MT value. That is to say, let $E_{300} = TT - MT$. Then, we obtain Table 3 below.

Table 3. Estimated E_{300} value.

RPM	TT	MT	E_{300}
500	61.375	52.991	8.384
1000	30.727	24.541	6.186
1500	20.490	15.357	5.133
2000	15.368	11.280	4.089
2500	12.295	8.528	3.767
3000	10.246	6.530	3.716
3500	8.783	5.301	3.481
4000	7.685	4.264	3.421
4500	6.831	3.920	2.911
5000	6.148	3.536	2.612
5500	5.589	2.801	2.788
6000	5.123	2.718	2.406

We then perform the curve estimate for the E_{300} value by using the SPSS. We will use the Logarithmic model and the Inverse model as selected in Step 1. The results of the analysis are as follows (Figure 2).

Model Summary and Parameter Estimates

Dependent Variable: E_300

Equation	Model Summary					Parameter Estimates	
	R Square	F	df1	df2	Sig.	Constant	b1
Logarithmic	.964	270.083	1	10	.000	21.830	-2.253
Inverse	.953	201.367	1	10	.000	2.412	3214.807

The independent variable is RPM.

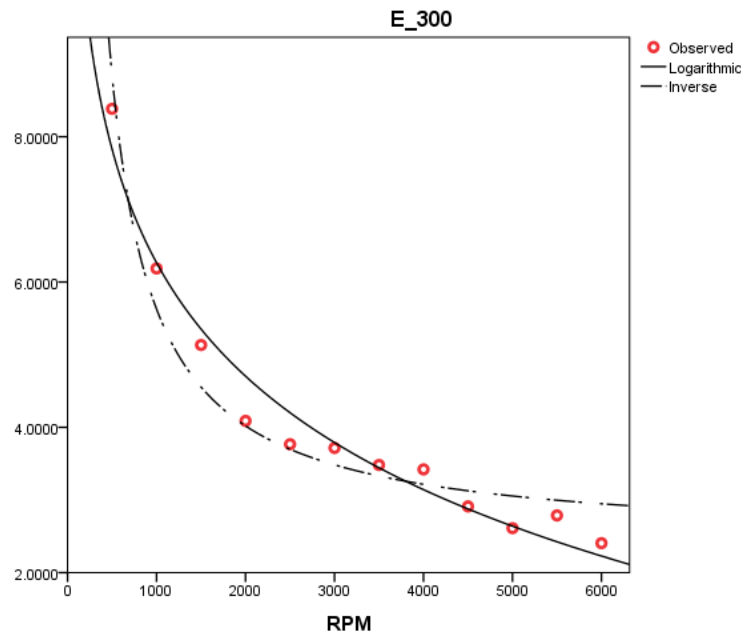


Figure 2. Curve estimation for E_{300} .

Thus, the estimated functions are given by the formulas

$$\text{Logarithmic : } h(\omega) = 21.83 - 2.253 \ln(\omega)$$

and

$$\text{Inverse : } h(\omega) = 2.41182 + \frac{3214.8068}{\omega}.$$

By using these functions, the estimated functions are given by the formulas

$$h_{log}(\omega) = \frac{1050}{\sqrt{1 + 0.00116671\omega^2}} - 21.83 + 2.253 \ln(\omega)$$

and

$$h_{inv}(\omega) = \frac{1050}{\sqrt{1 + 0.00116671\omega^2}} - 2.41182 - \frac{3214.8068}{\omega}.$$

All four estimated functions given are suitable for reducing time and cost in the spin-coating process. To reduce the difference further, the following comparisons are made. The data obtained by each functions are given by the following Table 4 below.

Table 4. Data obtained by each estimated functions.

RPM	TT	MT	h_{log}	h_{inv}
500	61.375	52.991	53.538	52.534
1000	30.727	24.541	24.462	25.100
1500	20.490	15.357	15.138	15.935
2000	15.368	11.280	10.665	11.349
2500	12.295	8.528	8.095	8.598
3000	10.246	6.530	6.456	6.763
3500	8.783	5.301	5.340	5.452
4000	7.685	4.264	4.543	4.469
4500	6.831	3.920	3.955	3.705
5000	6.148	3.536	3.510	3.093
5500	5.589	2.801	3.165	2.593
6000	5.123	2.718	2.895	2.176
R^2			0.964	0.953

The function that the best describes the measured thickness (MT) value among the functions derived in Steps 1 and 2 undergo several iterations until the smallest error (see Table 5) is achieved. Here, the sum of squares error (SSE) is given. The red value for each RPM represents the smallest difference.

Table 5. The smallest error.

RPM	MT- $h_{inverse}$	MT- h_{power}	MT- h_{log}	MT- h_{inv}
500	0.442	-3.885	-0.557	0.457
1000	-0.537	0.113	0.079	-0.560
1500	-0.563	0.457	0.219	-0.578
2000	-0.061	0.788	0.615	-0.069
2500	-0.066	0.536	0.434	-0.069
3000	-0.233	0.131	0.073	-0.233
3500	-0.153	-0.001	-0.039	-0.151
4000	-0.210	-0.243	-0.280	-0.206
4500	0.210	0.017	-0.035	0.215
5000	0.437	0.104	0.027	0.443
5500	0.201	-0.255	-0.364	0.208
6000	0.534	-0.031	-0.178	0.542
SSE	1.490	16.375	1.181	1.565

To test compliance, we decide to use function with the smallest SSE value to approximate MT value. It is

$$h_{t=300}(\omega) \equiv h_{log}(\omega) = \frac{1050}{\sqrt{1 + 0.00116671\omega^2}} - 21.83 + 2.253 \ln(\omega). \tag{8}$$

Step 3. We now establish the following hypothesis to test the function h_{log} and the consistency of MT value. Let μ_{MT} and μ_h be population means of MT values and the estimated function h_{log} , respectively. Then, we formulate the following research hypothesis.

$$H_0 : \mu_{MT} = \mu_h,$$

$$H_1 : \mu_{MT} \neq \mu_h.$$

To test this hypothesis, the results of the paired Samples *t*-test at a significant level $\alpha = 5\%$ are as follows (Figure 3).

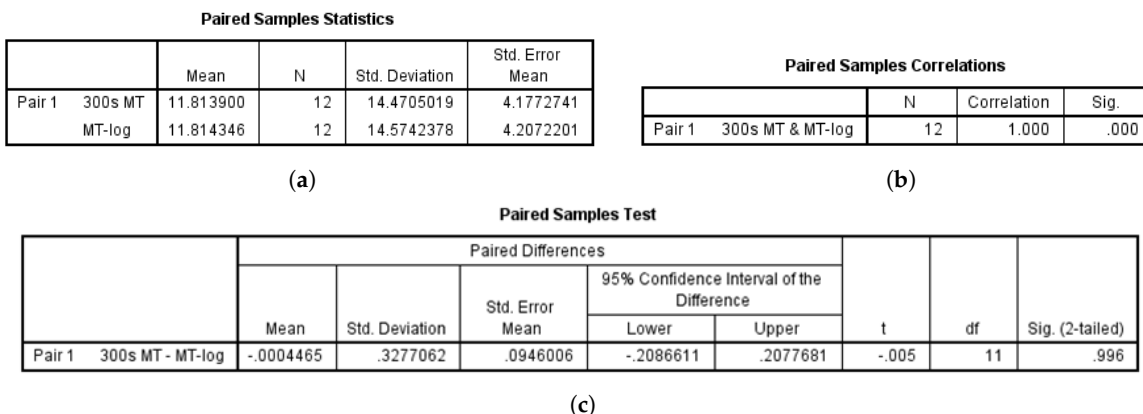


Figure 3. t-test.

Therefore, we accept the null hypothesis (H_0) to obtain the statistical basis for estimating h_{log} as an approximation of the MT value. From Steps 1 through 3, the best-estimated function corresponds to a fixed time of 300 s; i.e., the function given by Equation (8) is the best curve estimate for a fixed time of 300 s.

2.2. Fixed RPM at 1000

By the similar method as in Section 2.1, we can obtain the estimated function of the following case of fixed RPM at 1000. Then, the estimated function is given by the formula

$$h_{\omega=1000}(t) = \frac{1050}{\sqrt{1 + 3.889t}} - 22.2524 + 2.69 \ln(t).$$

We also can compare the TT value, the MT value and the estimated function value as the following Table 6.

Table 6. Compared values when there is fixed RPM 1000.

TIME	TT	MT	$h_{\omega=1000}$
100	53.176	43.269	43.311
200	37.625	29.576	29.625
300	30.727	24.541	23.818
400	26.613	19.710	20.478
500	23.905	18.192	18.270
600	21.731	16.591	16.687
700	20.121	15.948	15.490
800	18.822	14.431	14.551

The statistical hypothesis test of the estimated function $h_{\omega=1000}(t)$ is as follows. The results of the paired Sample t-test to verify the homogeneity of the two groups, as shown in Step 3 of Section 2.1, are as follows (Figure 4).

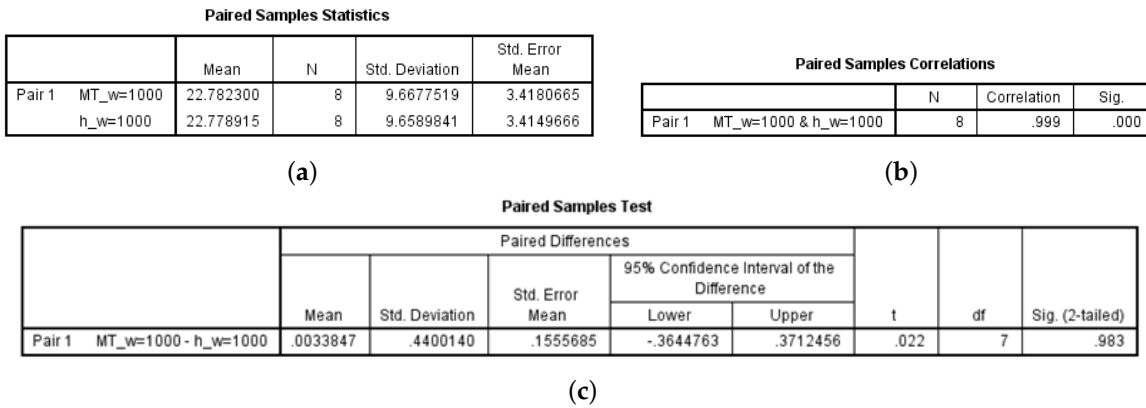


Figure 4. t-test.

Therefore, we have a statistical basis to conclude that populations in both sample spaces are equal to each other at a significant level $\alpha = 5\%$.

2.3. Other Cases

Through the process same as in cases 2.1 and 2.2 above, we obtain estimated functions for the time fixed at 450 and 600 s and the RPM fixed at 2000 and 3000. First, when the time is fixed at 450 and 600, we obtain estimated functions by setting the RPM as a variable as follows:

$$h_{t=450}(\omega) = \frac{1050}{\sqrt{1 + 0.00175\omega^2}} - 1.9398 - \frac{4346.44}{\omega}$$

and

$$h_{t=600}(\omega) = \frac{1050}{\sqrt{1 + 0.00233342\omega^2}} - 19.8476 + 2.104 \ln(\omega).$$

Table 7 is about the value of $MT_{t=450}$ and $MT_{t=600}$, and estimated function values.

Table 7. The thickness profile at $t = 450$ and $t = 600$.

RPM	$MT_{t=450}$	$h_{t=450}$	$MT_{t=600}$	$h_{t=600}$
500	38.969	39.510	36.454	36.664
1000	20.242	18.806	16.591	16.418
1500	11.639	11.894	10.177	10.029
2000	8.309	8.436	7.133	7.012
2500	6.134	6.361	4.996	5.309
3000	5.216	4.978	4.493	4.243
3500	4.199	3.990	3.580	3.532
4000	2.989	3.248	3.002	3.037
4500	2.199	2.672	2.478	2.681

Results of the t -test for estimated function values and MT values are as follows (in Figure 5), respectively.

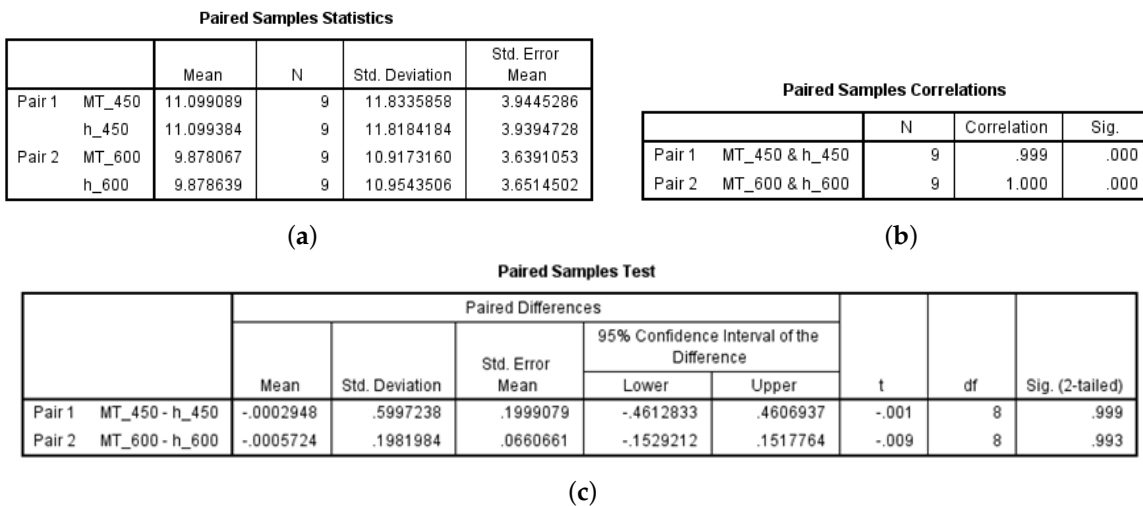


Figure 5. t-test.

Therefore, we see that the mean of populations of estimated functions and MT values are the same at a significant level $\alpha = 5\%$.

Next, when the RPM is fixed, we obtain estimated functions for the time parameter

$$h_{\omega=2000}(t) = \frac{1050}{\sqrt{1 + 15.5561t}} - 3.2594 - \frac{333.83446}{t}$$

and

$$h_{\omega=3000}(t) = \frac{1050}{\sqrt{1 + 35.00132t}} - 12.8084 + 1.60735 \ln(t).$$

We get $MT_{\omega=2000}$, $MT_{\omega=3000}$ and estimated values as shown in Table 8.

Table 8. The thickness profile at $\omega = 2000$ and $\omega = 3000$.

TIME	$MT_{\omega=2000}$	$h_{\omega=2000}$	$MT_{\omega=3000}$	$h_{\omega=3000}$
100	19.908	20.015	12.224	12.340
200	13.986	13.893	8.493	8.257
300	11.280	10.996	6.530	6.606
400	9.240	9.206	5.662	5.695
500	7.977	7.978	5.265	5.118
600	7.133	7.052	4.493	4.719
700	5.984	6.325	4.472	4.430
800	5.703	5.735	4.235	4.210

The results of the t-test are as follows (in Figure 6):

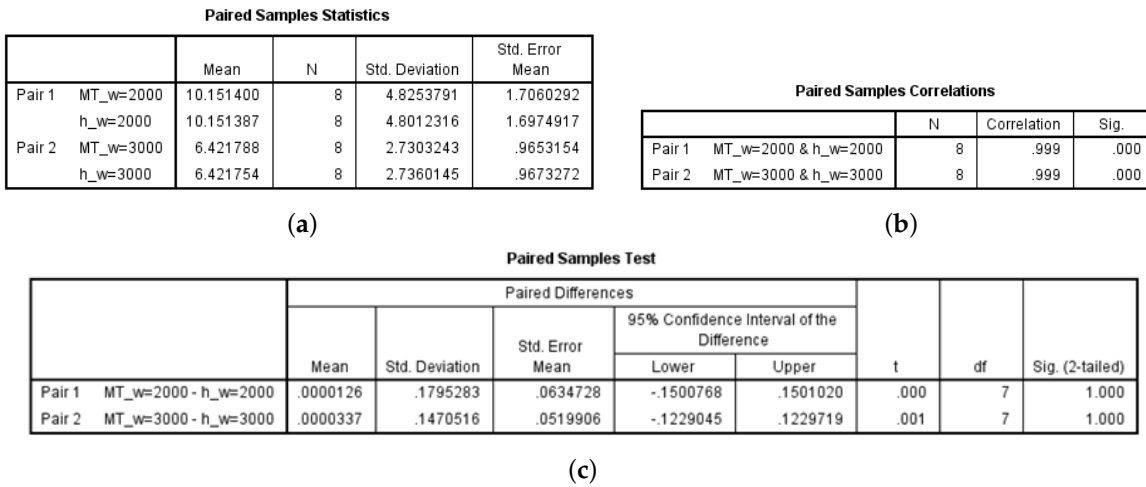


Figure 6. t-test.

In addition, we see that the mean of populations of estimated functions and MT values are the same at a significant level $\alpha = 5\%$.

2.4. Summary of Section 2

From Sections 2.1–2.3, we derived a curve-estimated function for each case. Figure 7 shows that all functions provided an estimate that was statistically equivalent to the MT values. These results suggest that the estimated function can be induced for other RPMs and times.

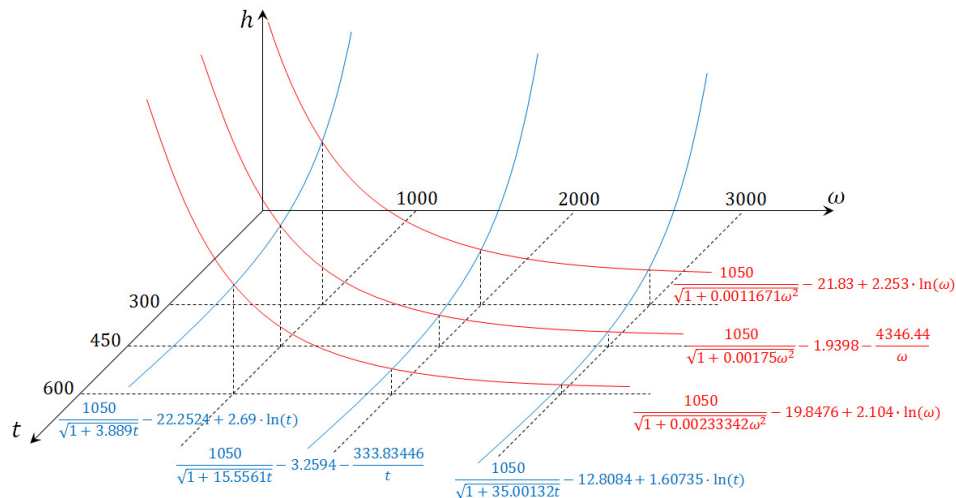


Figure 7. Six curve estimated functions.

3. A Modified Equation for Thickness of the Film Fabricated by Spin Coating via the Polyhedron Approximation

In Section 2, we obtained six estimated functions regarding t and ω . In this section, we are going to establish the polyhedron approximation with respect to the modified equation for thickness of the film fabricated by spin coating.

3.1. Polyhedron Approximation

We first take 13 points from a_1 to a_{13} via the estimated functions obtained in Section 2. Using these points, we can divide into 13 areas of the domain $D = \{(t, \omega) | 300 \leq t < \infty, 1000 \leq \omega < \infty\}$ as follows (Figure 8):

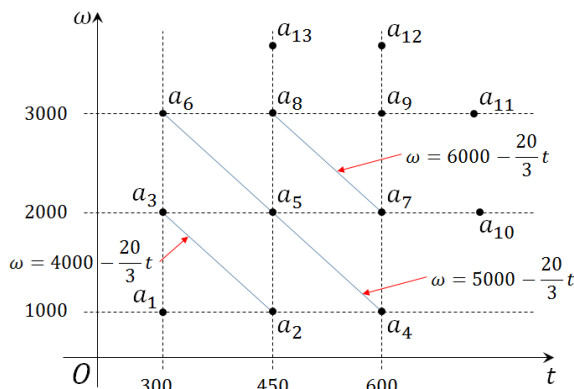


Figure 8. Separated domain.

Now, let $D_{i,j,k}$ be the sub-area of D with a_i, a_j and a_k as the vertex. Then, each area can be expressed in Table 9:

Table 9. Each sub-area of domain.

Sub-Area	Domain
$D_{1,2,3}$	$\{(t, \omega) 300 \leq t < 450, 1000 \leq \omega < 4000 - \frac{20}{3}t\}$
$D_{2,3,5}$	$\{(t, \omega) 300 \leq t < 450, 4000 - \frac{20}{3}t \leq \omega < 2000\}$
$D_{2,4,5}$	$\{(t, \omega) 450 \leq t < 600, 1000 \leq \omega < 5000 - \frac{20}{3}t\}$
$D_{3,5,6}$	$\{(t, \omega) 300 \leq t < 450, 2000 \leq \omega < 5000 - \frac{20}{3}t\}$
$D_{4,5,7}$	$\{(t, \omega) 450 \leq t < 600, 5000 - \frac{20}{3}t \leq \omega < 2000\}$
$D_{5,6,8}$	$\{(t, \omega) 300 \leq t < 450, 5000 - \frac{20}{3}t \leq \omega < 3000\}$
$D_{5,7,8}$	$\{(t, \omega) 450 \leq t < 600, 2000 \leq \omega < 6000 - \frac{20}{3}t\}$
$D_{7,8,9}$	$\{(t, \omega) 450 \leq t < 600, 6000 - \frac{20}{3}t \leq \omega < 3000\}$
$D_{4,7,10}$	$\{(t, \omega) 600 \leq t < \infty, 1000 \leq \omega < 2000\}$
$D_{7,9,11}$	$\{(t, \omega) 600 \leq t < \infty, 2000 \leq \omega < 3000\}$
$D_{9,11,12}$	$\{(t, \omega) 600 \leq t < \infty, 3000 \leq \omega < \infty\}$
$D_{8,9,12}$	$\{(t, \omega) 450 \leq t < 600, 3000 \leq \omega < \infty\}$
$D_{8,9,13}$	$\{(t, \omega) 300 \leq t < 450, 3000 \leq \omega < \infty\}$

Let A_i be the intersection of the function values of a_i for functions obtained in Section 2. We then split the graph of the two-parameter function into a plane passing through three points as shown below (Figure 9).

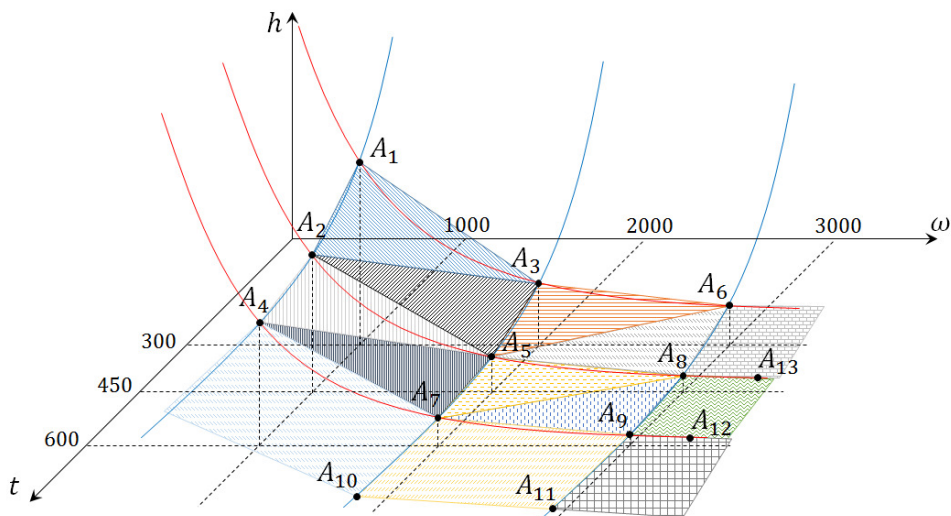


Figure 9. Planes.

Let $\Pi_{i,j,k}$ be the equation of plane passing through three points A_i, A_j and A_k . Then, all equations of the plane are as follows (Table 10).

Table 10. Equation of planes.

Plane	Equation
$\Pi_{1,2,3}$	$t + 0.391529\omega + 29.4118h - 1401.53 = 0$
$\Pi_{2,3,5}$	$t + 0.677312\omega + 64.2123h - 2349.91 = 0$
$\Pi_{2,4,5}$	$t + 0.635932\omega + 60.2894h - 2238.84 = 0$
$\Pi_{3,5,6}$	$t + 0.295985\omega + 64.2123h - 1547.26 = 0$
$\Pi_{4,5,7}$	$t + 0.977515\omega + 102.669h - 3276.9 = 0$
$\Pi_{5,6,8}$	$t + 0.36767\omega + 110.947h - 2127.51 = 0$
$\Pi_{5,7,8}$	$t + 0.340246\omega + 102.669h - 2002.36 = 0$
$\Pi_{7,8,9}$	$t + 0.548209\omega + 214.9h - 3207.38 = 0$
$\Pi_{4,7,10}$	$t + 1.46929\omega + 154.321h - 4623.61 = 0$
$\Pi_{7,9,11}$	$t + 1.89665\omega + 743.49h - 9620.82 = 0$
$\Pi_{9,11,12}$	$t + 1.07435\omega + 743.494h - 7153.9 = 0$
$\Pi_{8,9,12}$	$t + 0.31053\omega + 214.9h - 2494.34 = 0$
$\Pi_{6,8,13}$	$t + 0.214127\omega + 110.947h - 1666.86 = 0$

Let $h_{\Pi_{i,j,k}}(t, \omega)$ denote the new expression of plane with respect to t and ω . For example,

$$h_{\Pi_{1,2,3}}(t, \omega) = 47.652 - 0.0133\omega - 0.034t$$

and

$$h_{\Pi_{3,5,6}}(t, \omega) = 24.096 - 0.0043\omega - 0.0156t.$$

Using these, we obtain an approximate polyhedron function of the modified. Let

$$h_{\Pi}(t, \omega) = \sum_{i,j,k} h_{\Pi_{i,j,k}}(t, \omega) \chi_{D_{i,j,k}}, \tag{9}$$

where $\sum_{i,j,k}$ means adding all the possible circumstances in Table 10 above. The function $h_{\Pi}(t, \omega)$ is the polyhedron approximation of the equation for thickness of the film fabricated by spin coating.

3.2. Verification of the Polyhedron Approximation

In this section, we try to perform statistical verification of the polyhedron approximation obtained in Section 3.1. In order to do this, we first choose 14 points except a_j 's, denoted by b_j 's, in Figure 10. These points b_j are in the six curve estimation functions in Section 2. We are going to use these points to determine if the polyhedron function $h_{\Pi}(t, \omega)$ is an extension function with curve estimation functions.

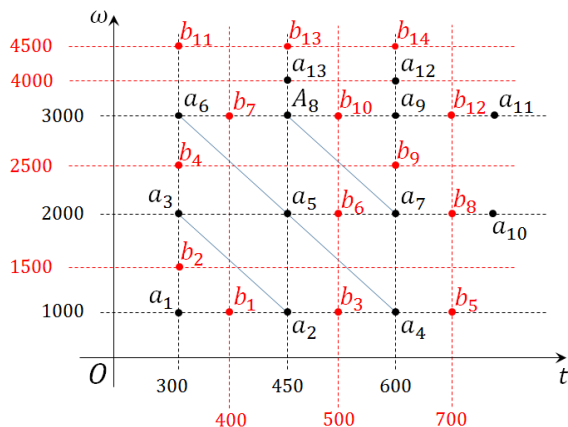


Figure 10. Add Points for the verification.

We then obtain the following Table 11 below.

Table 11. Compared values.

b_i	Coordinates	Curve _{appro}	$\Pi_{i,j,k}$	$h_{\Pi}(b_i)$
b_1	(400, 1000)	20.4781	$\Pi_{1,2,3}$	20.7520
b_2	(300, 1500)	15.1329	$\Pi_{1,2,3}$	17.5020
b_3	(500, 1000)	18.2702	$\Pi_{2,4,5}$	18.3349
b_4	(300, 2500)	8.0908	$\Pi_{3,5,6}$	8.6660
b_5	(700, 1000)	15.4906	$\Pi_{4,7,10}$	15.9110
b_6	(500, 2000)	7.9778	$\Pi_{5,7,8}$	8.0531
b_7	(400, 3000)	5.6956	$\Pi_{6,8,13}$	5.7239
b_8	(700, 2000)	6.3254	$\Pi_{4,7,10}$	6.8300
b_9	(600, 2500)	5.3086	$\Pi_{7,9,11}$	5.6600
b_{10}	(500, 3000)	5.1175	$\Pi_{8,9,12}$	5.0570
b_{11}	(300, 4500)	3.9517	$\Pi_{6,8,13}$	3.7739
b_{12}	(700, 3000)	4.4294	$\Pi_{9,11,12}$	4.5120
b_{13}	(450, 4500)	2.6720	$\Pi_{6,8,13}$	2.4239
b_{14}	(600, 4500)	2.6812	$\Pi_{9,11,12}$	2.5420

We can perform the statistical analysis to see whether the polyhedron approximation is correct. The results of the analysis are as follows (Figure 11):

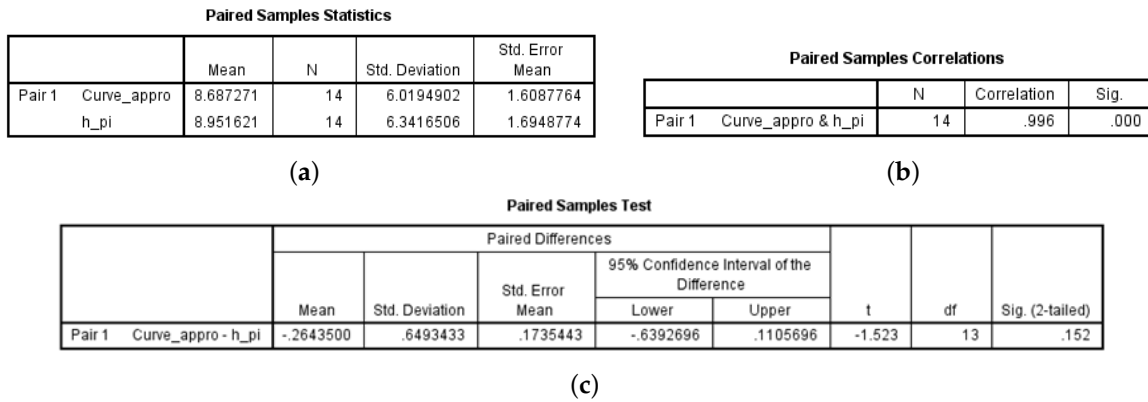


Figure 11. t-test.

This shows that the significance value 0.152 is greater than the significance level value 0.05. Therefore, we can not reject the null hypothesis $h_0 : \mu_{Curve_{appro}} = \mu_{h_{\Pi}}$. This means that values of $Curve_{appro}$ are statistically equal to values of h_{Π} .

3.3. Summary of Section 3

We took points from a_1 to a_{13} in the domain of $f_{\Pi}(t, \omega)$ using the six curves described in Section 2 to find the approximate function for the binary function $f(t, \omega)$. The domain was then divided into sub-areas $D_{i,j,k}$, passing through three points, a_i, a_j , and a_k . We obtained equations of planes $\Pi_{i,j,k}$ passing through A_i, A_j , and A_k , corresponding to the MT values of a_i, a_j , and a_k at each vertex of $D_{i,j,k}$, respectively. We then estimated the polyhedron approximation, $h_{\Pi}(t, \omega)$, as shown in Equation (9). To assess the suitability of the polyhedron approximation h_{Π} , we set 14 points of b_1, \dots, b_{14} in the domain D . The values listed in Table 12 were determined by substituting $Curve_{appro}$ and h_{Π} . Then, a paired sample t-test was performed between $Curve_{appro}$ and h_{Π} values, i.e., the curve approximation data from Section 2 and the data obtained by substituting the equation of polyhedron h_{Π} , respectively, to determine whether the mean was statistically identical within 5% of the significance level. Our results revealed that the polyhedron approximation h_{Π} contained six of the curves from Section 2; thus, our function provides a good approximation of the binary function $f(t, w)$.

4. Application: Target Verification

In this section, we try the target verification. We first set the target thickness and thus obtain the required time or RPM for each cases. Finally, we again conduct an experiment. The maximum rotation time for the Spin Coater ACE-200 is 999 s. Thus, the likelihood of error in the coating thickness estimations below 4 μm and above 20 μm is high.

The following table shows the results obtained by using the curve estimation function obtained in Section 2 when the RPM is fixed at $\omega = 1000, 2000$ and 3000, and the rotation time t is fixed at $t = 300, 450$ and 600, respectively (see Table 12).

Table 12. Compared values.

$h(\mu\text{m})$	ω	t	t	ω
4	1000	-	300	4453
	2000	1251	450	3493
	3000	925	600	3150
5	1000	-	300	3692
	2000	956	450	2990
	3000	526	600	2623
6	1000	-	300	3181
	2000	752	450	2613
	3000	360	600	2265
7	1000	-	300	2809
	2000	606	450	2321
	3000	269	600	2002
8	1000	6194	300	2522
	2000	498	450	2087
	3000	211	600	1799
9	1000	3007	300	2294
	2000	415	450	1896
	3000	171	600	1637
10	1000	2062	300	2106
	2000	350	450	1737
	3000	143	600	1503
15	1000	749	300	1511
	2000	174	450	1224
	3000	71	600	1078
20	1000	418	300	1187
	2000	100	450	945
	3000	44	600	846

With regard to Table 12, we discuss the thickness value for the parameters specified. When the RPM is fixed, there is no value at $\omega = 1000$, as shown in the table. Because the function $h_{\omega=1000}(t) = \frac{1050}{\sqrt{1+3.889t}} - 22.2524 + 2.69 \ln(t)$ has a local minimum value 7.847 at $t = 9793.59$, there is no value from 4 μm to 7 μm . Therefore, when a thickness of 4 μm to 7 μm is desired, a speed higher than 1000 RPM is required. Additionally, because the ACE-200 system has a maximum spin time of 999 s, it cannot provide a thickness in the desired range of 8 μm to 10 μm when $\omega = 1000$. We give the following summary in Table 13:

Table 13. Suitable RPM with fixed rotation time.

Target Thickness (μm)	Suitable RPM
11–20	less than 1000
7–10	1000–3000
4–6	more than 3000

In another experiment, the rotation time t is held fixed at $t = 300, 450$ and 600 s. To obtain the desired thickness, as shown in Table 12, the RPM could be adjusted for the fixed time frame. In contrast to the previous case in which the RPM was fixed, here we are able to adjust the RPM to produce the desired

thickness within the allowable range, given a fixed rotation time. Therefore, it appears to be more effective to fix the rotation time t to obtain the target film thickness in spin coating processes.

Table 14 lists the thicknesses determined by substituting RPM for the rotation time t for each coating thickness into h_{II} from Section 3. To compare these values with MT values, we prepare three samples in which the rotation time is fixed at 450 s. The $MT_{t=450}$ values in the following table represent the average values of the raw data of the three samples.

Table 14. RPMs for the target thickness, polyhedron values and MT value.

$h(\mu\text{m})$	t	ω	$h_{II}(\mu\text{m})$	$MT_{t=450}(\mu\text{m})$
4	300	4453	3.863	3.777
	450	3493	4.602	
	600	3150	4.432	
5	300	3692	5.309	4.956
	450	2990	5.271	
	600	2623	5.340	
6	300	3181	6.280	6.058
	450	2613	6.515	
	600	2265	6.271	
7	300	2809	7.337	6.390
	450	2321	7.479	
	600	2002	6.955	
8	300	2522	8.571	7.481
	450	2087	8.251	
	600	1799	8.981	
9	300	2294	9.552	8.587
	450	1896	9.757	
	600	1637	10.510	
10	300	2106	10.360	9.723
	450	1737	11.426	
	600	1503	11.783	
15	300	1511	17.356	15.163
	450	1224	16.813	
	600	1078	15.820	
20	300	1187	21.665	21.872
	450	945	—	
	600	846	—	

Actually, this result indicates that the results in Sections 2 and 3 and the values observed by the experiment are the same within the margin of error.

5. Conclusions

5.1. Importance of Results and Formulas in This Paper

Spin coating technology is useful in modern industrial society. However, it still relies on Formula (7), which was introduced in the 1950s, to determine spin coating film thickness. This conventional approach requires extensive time and experimentation to obtain the desired coating thickness, which increases costs. Here, we propose an alternative to this conventional approach. Using the function h_{II} , we can estimate the desired coating thickness given the rotation time and RPM, according to the conditions of the coating device. The coating thicknesses achieved using the proposed approach were within the error

range expected. In an example described in Section 4, we were able to obtain the coating thickness based on a fixed rotation time and RPM, using the six functions developed in Section 2. Additionally, the binary function $h_{\Pi}(t, \omega)$ estimated in Section 3 allows users to simulate the desired thickness without having to perform an actual experiment. As a result, many spin coating companies will save time and money using the method implemented in this study.

5.2. Another Approach

Our original goal was to express the equation for thickness of the film fabricated by spin coating as a new binary function. In Section 2, curved estimates were determined for each fixed variable, and, in Section 3.1, an approximation of the polyhedron function was acquired through the plane approximation method. In the next research work, we will attempt to obtain an approximation of the equation for thickness of the film fabricated by spin coating as a binary function of the curved estimate and polyhedron function. In Section 3, we split the domain D using points a_1 through a_{13} . Using a similar method, we obtained the function h_{Π_n} with n -splitting points. Then, $h_{\Pi} \equiv h_{\Pi_{13}}$. By adding more splitting points, we can derive the function $f(t, \omega)$ as the limit of $h_{\Pi_n}(t, \omega)$. That is,

$$h(t, \omega) = \lim_{n \rightarrow \infty} h_{\Pi_n}(t, \omega).$$

5.3. Expected Results

In this study, we estimated the bivariate function $h(t, \omega)$ by assuming rotation time and RPM as independent variables, while the other factors remained fixed. However, the factors affecting the actual coating thickness are h_0 , ρ , and μ . Thus, the addition of other variables to the function formula should improve the accuracy of the spin coating thickness prediction. Considering all of the factors that affect thickness would make the formula too complex, but given that spin coating companies use fixed coating materials, ρ and μ can be considered constants.

Therefore, in future studies, we will attempt to estimate a three-variable function $h(t, \omega, h_0)$ by setting the independent variables t , ω , and h_0 .

5.4. Capture of the Thickness Calculator by the Excel Program

Based on the results of this study, we developed a thickness calculator using the Microsoft Office Excel program (Microsoft Corp., Redmond, WA, USA). Here, we show screen shots of the initial screen and application screen of the calculator. This calculator can predict the thickness without actual experimentation. As you can see in Figures 12–14 below, they are shown for $t = 150$ and $\omega = 2700$. We will supply our calculator to companies free of charge, in order to help them achieve the desired coating thickness in spin coating processes.

	t	RPM	Thickness
Input 1			
Input 2			
Input 3			
Input 4			
Input 5			

(a) Initial screen

	t	RPM	Thickness
Input 1	300	4453	3.8632
Input 2	450	2613	6.5152
Input 3	600	1637	10.5095
Input 4	350	2700	7.1159
Input 5			

(b) Application screen

Figure 12. Calculator for t and RPM.

300s	RPM	Thickness	450s	RPM	Thickness	600s	RPM	Thickness
Input 1			Input 1			Input 1		
Input 2			Input 2			Input 2		
Input 3			Input 3			Input 3		
Input 4			Input 4			Input 4		
Input 5			Input 5			Input 5		

(a) Initial screen

300s	RPM	Thickness	450s	RPM	Thickness	600s	RPM	Thickness
Input 1	1000	24.46029	Input 1	500	39.50965	Input 1	500	36.664
Input 2	1500	15.1363	Input 2	1500	11.89365	Input 2	1000	16.418
Input 3	4000	4.541358	Input 3	2700	5.746266	Input 3	2000	7.012
Input 4	5000	3.507187	Input 4			Input 4		
Input 5			Input 5			Input 5		

(b) Application screen

Figure 13. Calculator for RPM.

RPM=1000	t	Thickness	RPM=2000	t	Thickness	RPM=3000	t	Thickness
Input 1			Input 1			Input 1		
Input 2			Input 2			Input 2		
Input 3			Input 3			Input 3		
Input 4			Input 4			Input 4		
Input 5			Input 5			Input 5		

(a) Initial screen

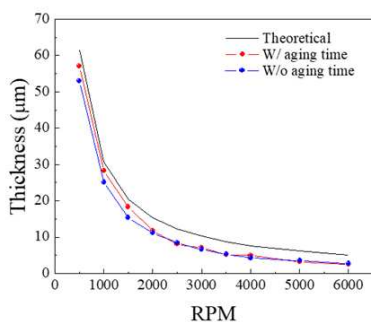
RPM=1000	t	Thickness	RPM=2000	t	Thickness	RPM=3000	t	Thickness
Input 1	100	43.31114	Input 1	100	26.69229	Input 1	200	8.256618
Input 2	150	34.6625	Input 2	200	17.23127	Input 2	300	6.605844
Input 3	200	29.62506	Input 3	300	13.22189	Input 3	500	5.117528
Input 4	250	26.25746	Input 4	350	11.92311	Input 4	550	4.901383
Input 5	400	20.47807	Input 5			Input 5		

(b) Application screen

Figure 14. Calculator for t.

We finish this paper by giving a remark.

Remark 2. We are working on data at fixed conditions of 300 s, as well as different times or fixed RPM conditions, and we will do further research. As shown in Figure 15 below, the experiment was conducted under different conditions, and it was confirmed that the thickness was changed due to the parameters that were not considered in the existing equation. For example, when the aging time is given after spin coating for a fixed condition of 300 s, the thickness changes as shown in the attached figure and the equation, and the equation obtained through curve estimation also changes. In addition, it is expected that process conditions for the manufacture of the desired thickness can be derived simply. In addition, it will be possible to apply to other materials, and further experiments are planned.



without aging time (at 300 s)

$$h = \frac{1050}{\sqrt{1+0.00116671\omega^2}} - 21.83 + 2.253 \ln(\omega)$$

with aging time (at 300 s)

$$h = -2.885 + \frac{30210.1512}{\omega}$$

Figure 15. Further research.

Author Contributions: Conceptualization, H.S.C. and W.-B.K.; method-ology, H.S.C.; software, U.G.L.; validation, D.H.H., and W.-B.K.; formal analysis, H.S.C. and U.G.L.; data curation, D.H.H.; writing–original draft preparation, H.S.C.

Funding: This research was supported by the Basic Science Research Program through the National Research Foundation of Korea (NRF) funded by the Ministry of Science, ICT and Future Planning (2017R1E1A1A03070041). The APC was funded by 2017R1E1A1A03070041.

Conflicts of Interest: The authors declare no conflict of interest.

References

1. Emslie, A.G.; Bonner, F.T.; Peck, L.G. Flow of a viscous liquid on a rotating disk. *J. Appl. Phys.* **1958**, *29*, 858–862. [[CrossRef](#)]
2. Huang, Y.-Y.; Chou, K.-S. Studies on the spin coating process of silica films. *Ceram. Int.* **2003**, *29*, 485–493. [[CrossRef](#)]
3. Sahu, N.; Parija, B.; Panigrahi, S. Fundamental understanding and modeling of spin coating process: A review. *Indian J. Phys.* **2009**, *83*, 493–502. [[CrossRef](#)]
4. Tyona, M. A theoretical study on spin coating technique. *Adv. Mater. Res.* **2013**, *2*, 195–208. [[CrossRef](#)]
5. Chang, C.-C.; Pai, C.-L.; Chen, W.-C.; Jenekhe, S.A. Spin coating of conjugated polymers for electronic and optoelectronic applications. *Thin Solid Films* **2005**, *479*, 254–260. [[CrossRef](#)]
6. Flack, W.W.; Soong, D.S.; Bell, A.T.; Hess, D.W. A mathematical model for spin coating of polymer resists. *J. Appl. Phys.* **1984**, *56*, 1199–1206. [[CrossRef](#)]
7. Jenekhe, S.A.; Schuldt, S.B. Coating flow of non-Newtonian fluids on a flat rotating disk. *Ind. Eng. Chem. Fund.* **1984**, *23*, 432–436. [[CrossRef](#)]
8. Norrman, K.; Ghanbari-Siahkali, A.; Larsen, N. 6 Studies of spin-coated polymer films. *Annu. Rep. Sect. C (Phys. Chem.)* **2005**, *101*, 174–201. [[CrossRef](#)]
9. Schwartz, L.W.; Roy, R.V. Theoretical and numerical results for spin coating of viscous liquids. *Phys. Fluids* **2004**, *16*, 569–584. [[CrossRef](#)]
10. Shimoji, S. Numerical analysis of the spin-coating process. *J. Appl. Phys.* **1989**, *66*, 2712–2718. [[CrossRef](#)]
11. Vorotilov, K.; Petrovsky, V.; Vasiljev, V. Spin coating process of sol-gel silicate films deposition: Effect of spin speed and processing temperature. *J. Sol-Gel Sci. Technol.* **1995**, *5*, 173–183. [[CrossRef](#)]
12. Yonkoski, R.; Soane, D. Model for spin coating in microelectronic applications. *J. Appl. Phys.* **1992**, *72*, 725–740. [[CrossRef](#)]
13. Natsume, Y.; Sakata, H. Zinc oxide films prepared by sol-gel spin-coating. *Thin Solid Films* **2000**, *372*, 30–36. [[CrossRef](#)]
14. Shih, T.-K.; Chen, C.-F.; Ho, J.-R.; Chuang, F.-T. Fabrication of PDMS (polydimethylsiloxane) microlens and diffuser using replica molding. *Microelectron. Eng.* **2006**, *83*, 2499–2503. [[CrossRef](#)]
15. Pavlidis, M.; Dimakopoulos, Y.; Tsamopoulos, J. The effect of viscoelastic properties under creeping flow. *J. Non-Newton. Fluid Mech.* **2010**, *165*, 576–591. [[CrossRef](#)]
16. Lindner, A.; Bonn, D.; Meunier, J. Viscous fingering in a shear-thinning fluid. *Phys. Fluids* **2000**, *12*, 256–261. [[CrossRef](#)]
17. Hogg, R.V.; McKean, J.W.; Craig, A.T. *Introduction to Mathematical Statistics*, 7th ed.; Pearson Education, Inc.: New York, NY, USA, 2013.
18. Weinberg, G.H.; Schumaker, J.A. *Statistics an Intuitive Approach*, 2nd ed.; Books/Cole Publishing Company, Inc.: Herndon, VA, USA, 1969.



© 2019 by the authors. Licensee MDPI, Basel, Switzerland. This article is an open access article distributed under the terms and conditions of the Creative Commons Attribution (CC BY) license (<http://creativecommons.org/licenses/by/4.0/>).